Science Advances
AAAS

Supplementary Materials for

RNA binding protein RBM46 regulates mitotic-to-meiotic transition in spermatogenesis

Baomei Qian *et al.*

Corresponding author: Lan Ye, lanye@njmu.edu.cn; Jian Zhou, jianzhou@njmu.edu.cn; Mingyan Lin, linmingyan@njmu.edu.cn

Sci. Adv. **8**, eabq2945 (2022)
DOI: 10.1126/sciadv.abq2945

This PDF file includes:

SUPPLEMENTARY MATERIALS

A

P12 WT YTHDC2 IP-MS targets

Enriched GO biological precess terms	*P-value*
mRNA processing (GO:0006397)	1.50E-45
ribonucleoprotein complex biogenesis (GO:0022613)	4.57E-43
RNA splicing, via transesterification reactions (GO:0000375)	1.21E-36
regulation of mRNA metabolic process(GO:1903311)	4.76E-29
RNA localization (GO:0006403)	6.67E-27
RNA transport (GO:0050658)	1.98E-22
mRNA catabolic process(GO:0006402)	1.63E-19
ncRNA processing(GO:0034470)	3.50E-17

B

P21 WT YTHDC2 IP-MS targets

Enriched GO biological precess terms	*P-value*
mRNA processing (GO:0006397)	1.33E-59
RNA splicing (GO:0008380)	4.18E-57
ribonucleoprotein complex biogenesis (GO:0022613)	2.58E-51
ribonucleoprotein complex assembly (GO:0022618)	3.15E-46
regulation of mRNA metabolic process (GO:1903311)	1.29E-35
regulation of translation (GO:0006417)	2.86E-35
RNA localization (GO:0006403)	3.94E-31

C

P21 WT YTHDC2 IP-MS

Protein identified	Unique peptides
YTHDC2-IP	
YTHDC2	57
MEIOC	44
UPF1	29
DDX4	20
PABPC1	19
MOV10	18
CNOT1	14
RBM46	13
CNOT10	10
CNOT9	4

Fig. S1. Mass spectrometry analysis of YTHDC2 immunoprecipitated complexes from P21 mouse testes. (A) Gene ontology analysis of RBM46 interactors in mouse testes at P12. (B) GO analysis of RBM46 interactors in mouse testes at P21. (C) Selective YTHDC2-associated protein candidates identified by mass spectrometry analysis from P21 mouse testes (n=5).

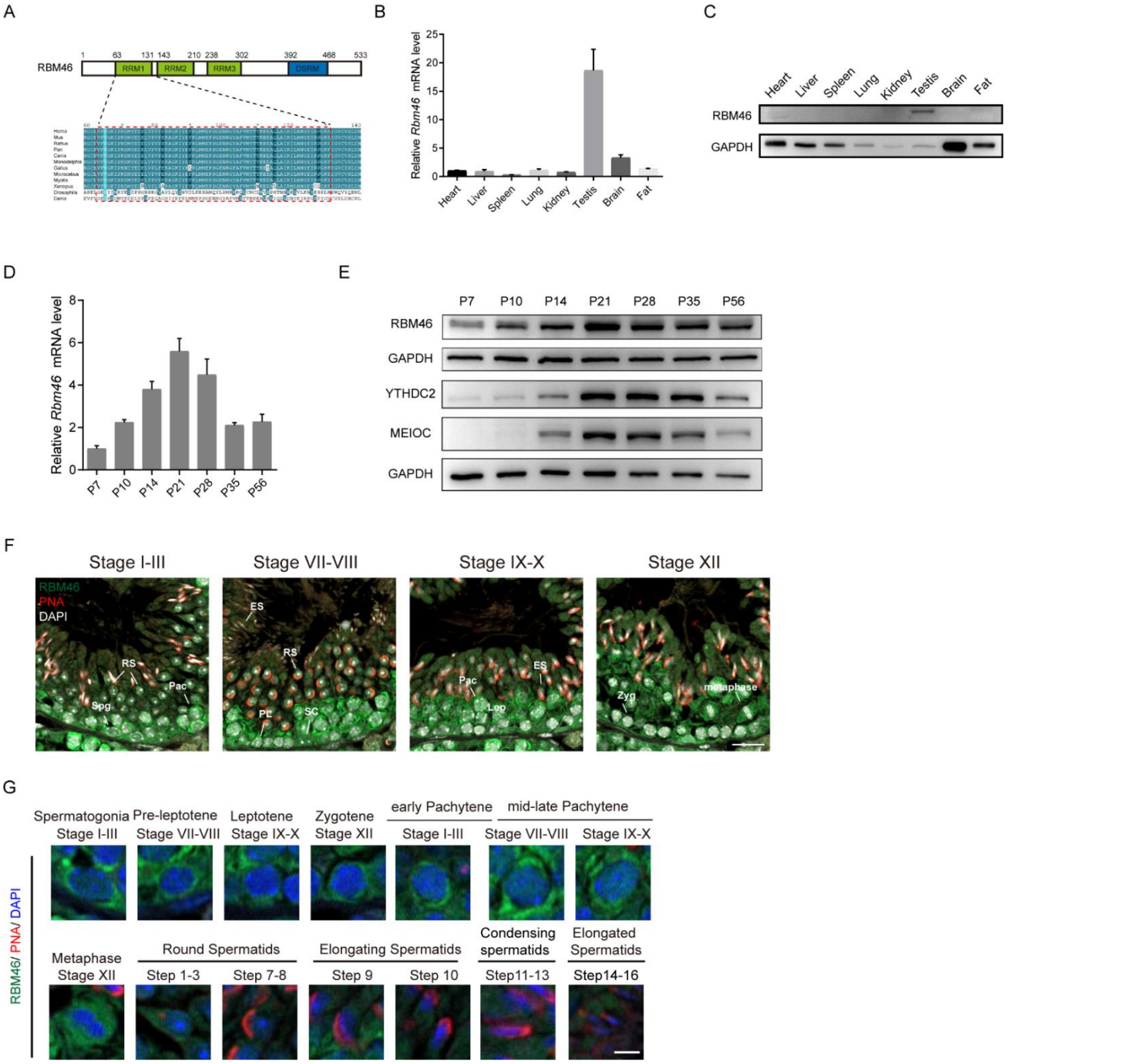

Fig. S2. *Rbm46* is a conserved gene and its expression increases at the onset of meiosis. (A) Schematic representation of RBM46 protein structure. The mouse *Rbm46* gene contains 5 exons. The RNA binding domains (green boxes) are highly conserved, and RRM1 is indicated by dotted lines. Represented species are as follows: Homo sapiens; mouse, musculus; Rattus norvegicus; Pan troglodytes; Canis; Monodelphis domestica; Gallus gallus; Microcebus murinus; Myotis brandtii ; Xenopus tropicalis; Drosophila melanogaster; Danio. (B-C) *Rbm46* mRNA transcripts and its protein abundance were evaluated by qRT-PCR (B) and western blot (C) in various tissues from adult mice. (D) Quantitative RT-PCR analysis of *Rbm46* transcripts in mouse testes at indicated time points. (E) Western blot analysis of RBM46, YTHDC2, and MEIOC during spermatogenesis. GAPDH serves as a loading control. (F-G) Immunofluorescence for RBM46 (green), PNA (red) and DAPI (blue) in adult wild-type testis sections. PNA is an acrosome marker. DNA was counterstained with DAPI. Scale bars: 20 μm. Lower panels show magnification image of single cell in the upper panels. Scale bars: 5 μm. Abbreviations: Spg, spermatogonia; PL, pre-leptotene; Lep, leptotene; Zyg, zygotene; Pac, pachytene; RS, round spermatids; ES, elongating spermatids.

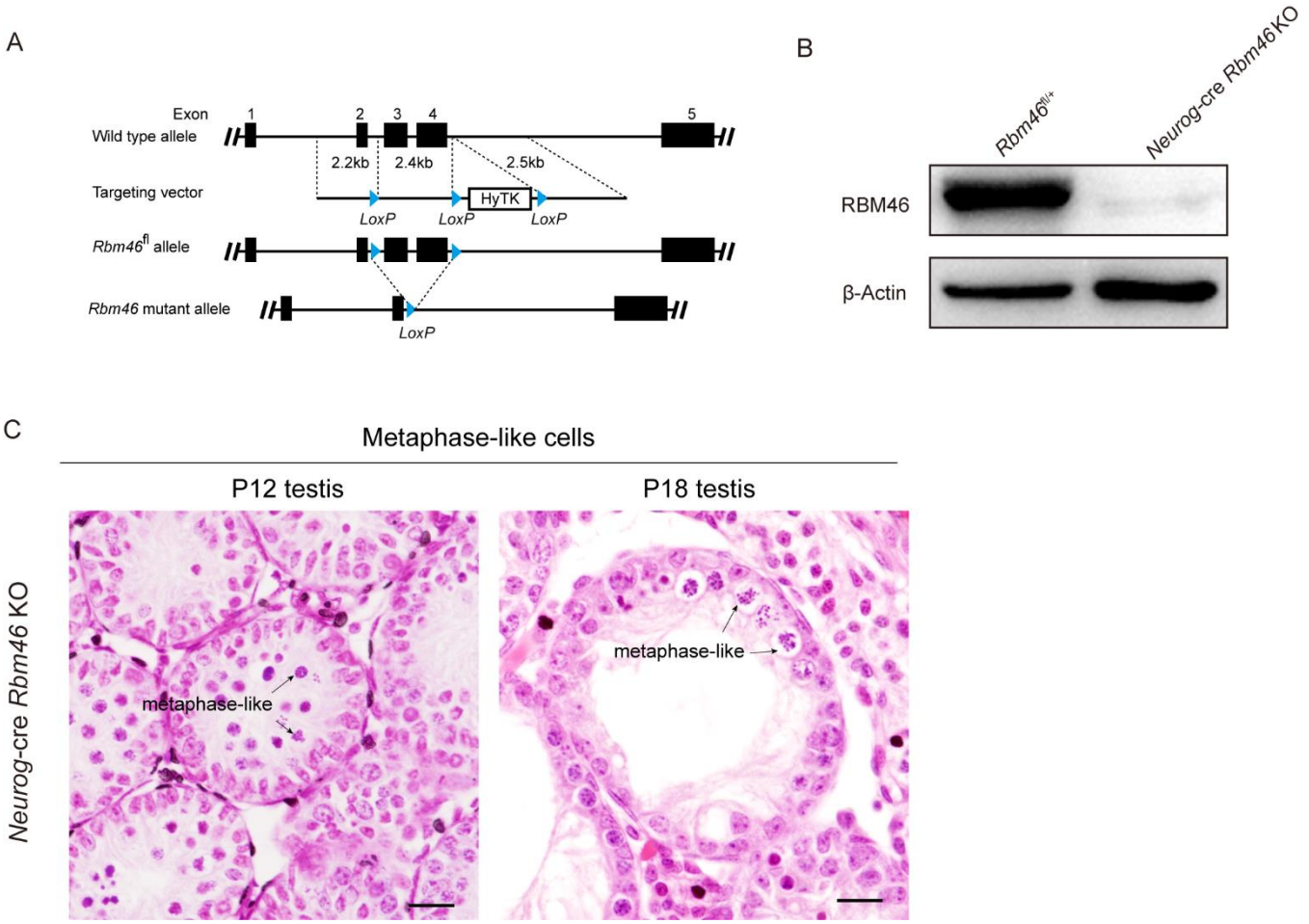

Fig. S3. Generation of testis-specific *Rbm46* knockout mice. (A) Genetic strategy for targeted disruption of *Rbm46* gene in mouse testis. *LoxP* sites were inserted into the intron 2 and intron 4 for flanking exon 3 and exon 4, which contain the putative RNA recognition motifs and RNA binding domains. Testis-specific deletion of *Rbm46* was achieved by breeding *Rbm*46$^{fl/+}$ to *Neurog*-cre transgenic mice. (B) Western blot analysis of RBM46 protein abundance in P21 wild-type and *Neurog*-cre *Rbm46* KO testis. (C) Metaphase-like cells with condensed chromosomes were observed *Neurog*-cre *Rbm46* KO testes at P12 and P18. Scale bar, 20 μm.

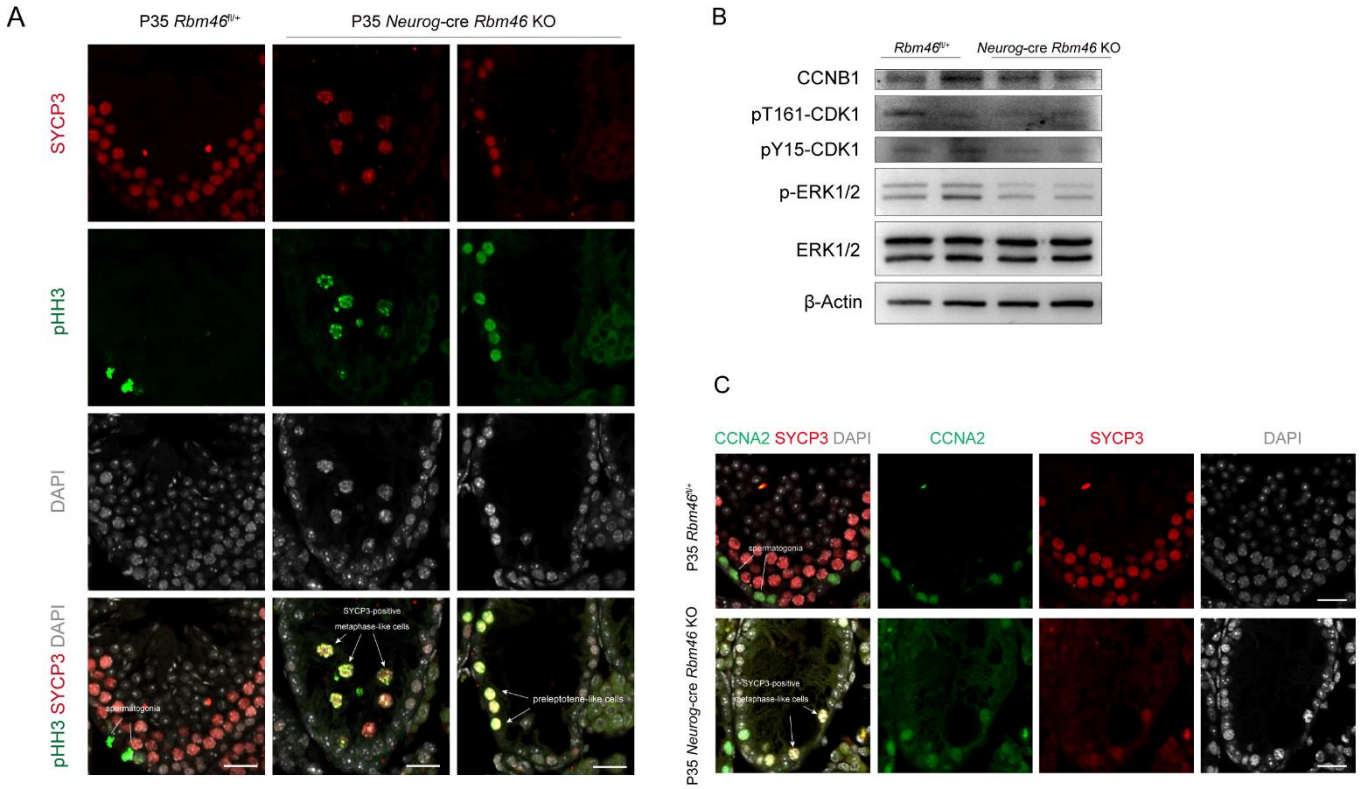

Fig. S4. *Rbm46* knockout does not affect the maturation-promoting factor complex, a Cyclin-CDK complex that promotes metaphase transition. (A) Frozen sections from P35 wild-type and *Neurog*-cre *Rbm46* KO testes were immunostained with pHH3 and SYCP3. (B) Western blot of testes lysates from wild-type and *Neurog*-cre *Rbm46* KO with the indicated antibodies. pT161-CDK1, phosphorylation of CDK1 at Thr161; pY15-CDK1, phosphorylation of CDK1 at Tyr15. (C) Immunofluorescence analysis with SYCP3 and CCNA2 antibodies on testis sections prepared from P35 WT and *Neurog*-cre *Rbm46* KO. Metaphase-like cells that express CCNA2 are indicated by arrows. Scale bar, 20 μm.

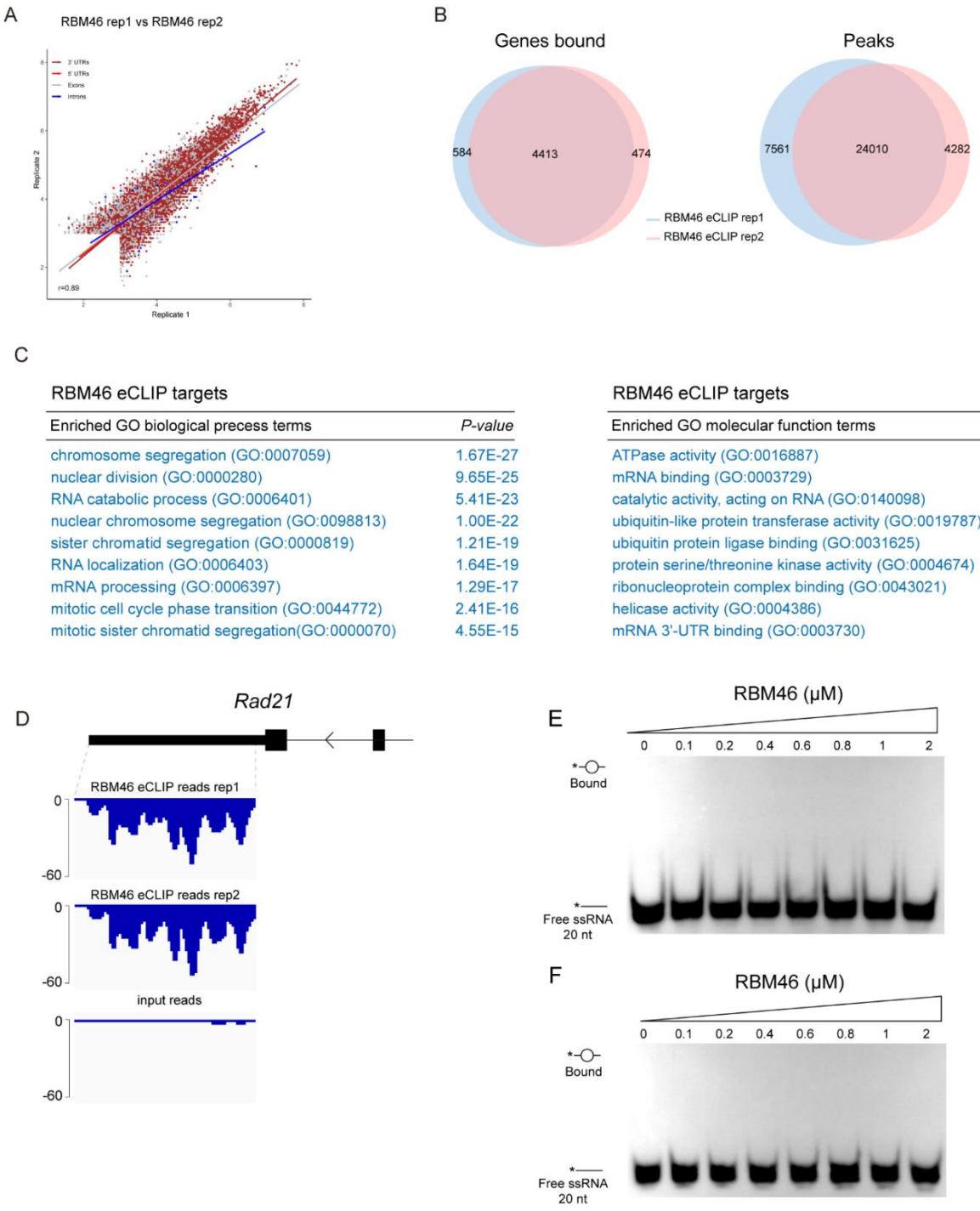

Fig. S5. **RBM46 preferentially binds mitotic-cell-cycle-related transcripts.** (A) Scatter plot indicating correlation (r=0.89) between region-based fold enrichment of RBM46 eCLIP-seq across biological duplicates. (B) Overlap between RBM46 peaks and its target genes from biologically two RBM46 eCLIP-seq replicates. RBM46 binding peaks were identified using a stringent parameter ($P \leq 0.001$, fold change ≥ 8). (C) GO biological process and molecular function terms of the top 50% RBM46 targets by eCLIP-seq in testis ($P \leq 0.001$, fold change ≥ 8). (D) Genome browser tracks showing RBM46 eCLIP-seq reads mapped to the 3' UTRs of the mitotic *Rad21* transcripts. (E) EMSA analysis of purified RBM46 protein with a 5' end-labelled single strand RNA probe (ssRNA) without RBM46 binding motif. This 20 nt synthetic ssRNA does not contain the RBM46 binding motif, and its sequence is from *Ccna2* 3' UTR. (F) EMSA experiments show that RBM46 protein doesn't bind a U-rich RNA sequence.

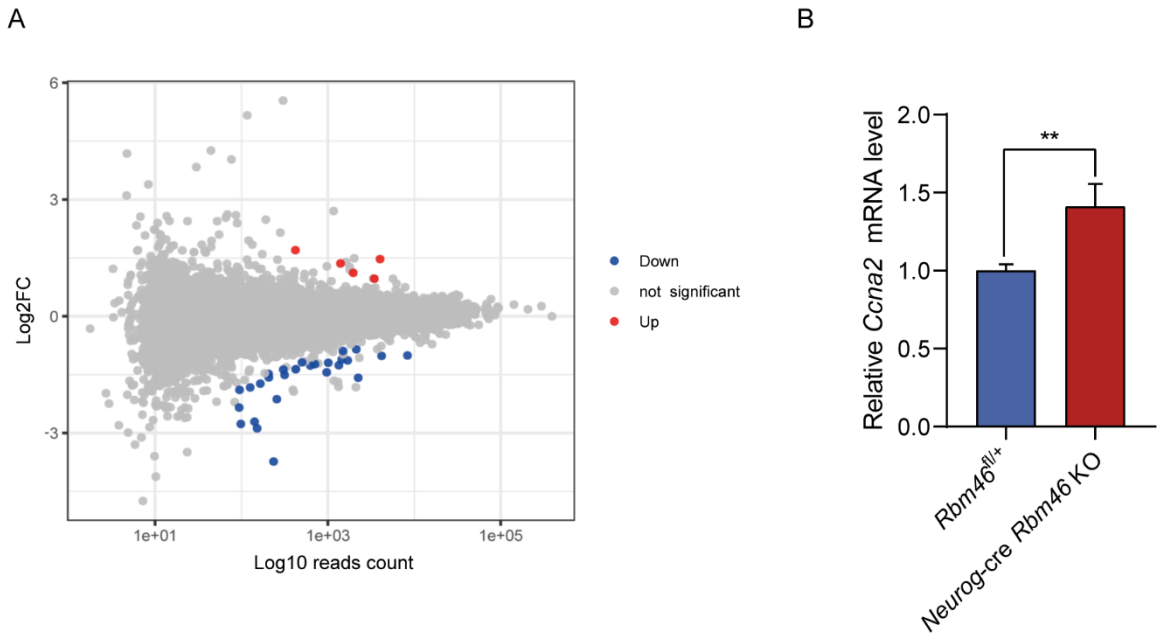

Fig. S6. **Transcriptomic analysis of wild-type and *Neurog*-cre *Rbm46* KO testes.** (A) RNA-seq analysis of differentially expressed genes in wild-type and *Neurog*-cre *Rbm46* KO testes at P10, when germ cells just enter meiosis. The upregulated and downregulated genes ($p < 0.05$, fold change >1.5) are shown as red dots and blue dots, respectively. Experiments were performed in biological duplicates. (B) *Ccna2* mRNA transcript levels in wild-type and *Neurog*-cre *Rbm46* KO testes at P14. n=3 for each genotype. ** $P < 0.01$, Student's t test.

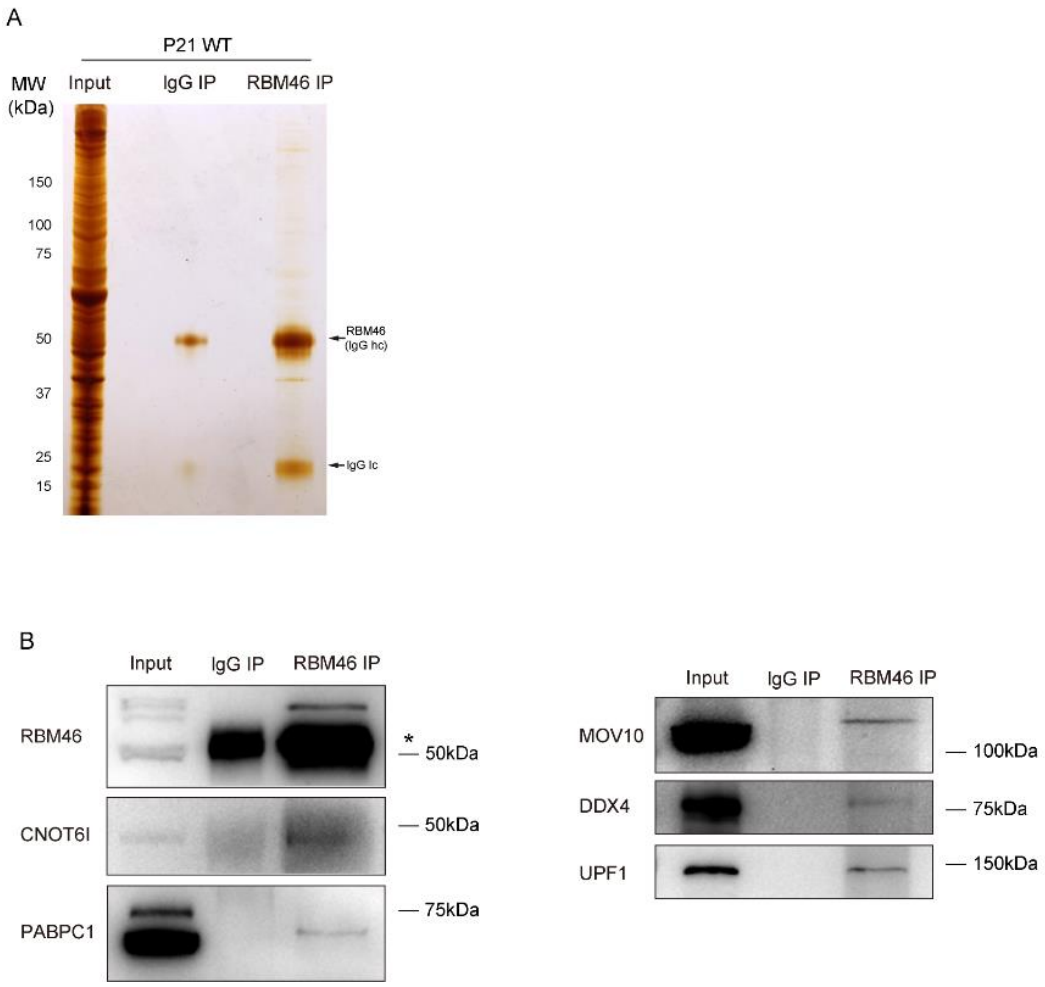

Fig. S7. RBM46 interacts with P-body components and post-transcriptionally regulates mitotic transcripts. (A) Identification of RBM46-associating partners by immunoprecipitation experiments either with RBM46 or normal IgG antibodies from mouse testes at P12 and P21. Immunoprecipitated RBM46 protein complexes were separated by SDS-PAGE, and the gel image stained with silver is selectively shown. Testis lysates were prepared from mouse at P12 (n=8) and P21 (n=5). (B) Immunoprecipitation of RBM46 from mouse testes lysates at P21 and western blot with P-body components, including MOV10, CNOT6l, DDX4, PABPC1, and the nonsense-mediated mRNA decay regulator UPF1.

A

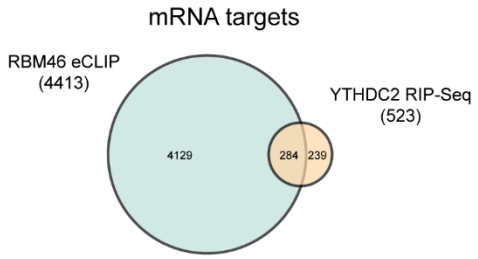

B

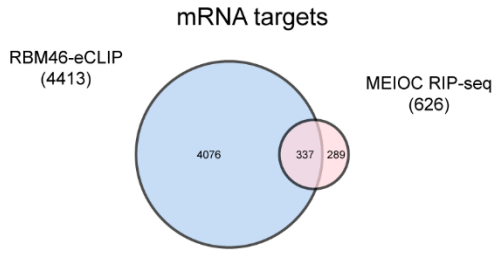

C

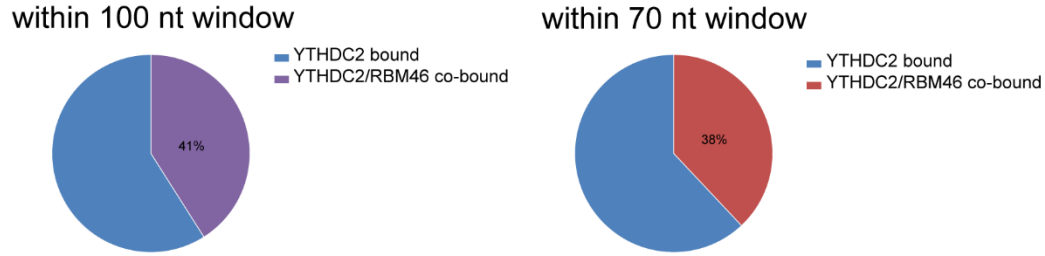

D

RBM46 and YTHDC2 shared targets

Enriched GO biological precess terms	*P-value*
RNA catabolic process (GO:0006401)	2.73E-07
ribonucleoprotein complex biogenesis (GO:0022613)	4.66E-06
regulation of RNA stability (GO:0043487)	5.04E-06
ncRNA metabolic process (GO:0034660)	1.07E-05
chromosome segregation (GO:0007059)	1.94E-05
nuclear chromosome segregation (GO:0098813)	2.21E-05
positive regulation of protein ubiquitination (GO:0031398)	5.55E-05
regulation of cell cycle phase transition (GO:1901987)	5.87E-05

Enriched GO molecular function terms	*P-value*
mRNA 3'-UTR binding (GO:0003730)	6.31E-08
mRNA binding (GO:0003729)	4.47E-07
poly(A) binding (GO:0008143)	1.36E-04
miRNA binding (GO:0035198)	1.68E-04
poly-purine tract binding (GO:0070717)	2.91E-04
regulatory RNA binding (GO:0061980)	4.94E-04
ATPase activity (GO:0016887)	6.25E-04
phosphatidylinositol-3-phosphatase activity(GO:0004438)	1.47E-03

E

YTHDC2 U-rich motifs by iCLIP-seq

Motif	*P-value*
	1E-133
	1E-59

F

Top motifs flanking RBM46 motif within 100 nt

Motif	*P-value*
	1E-689
	1E-23
	1E-23

G

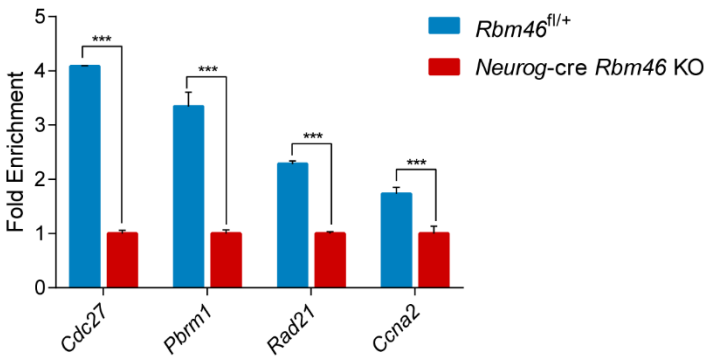

H

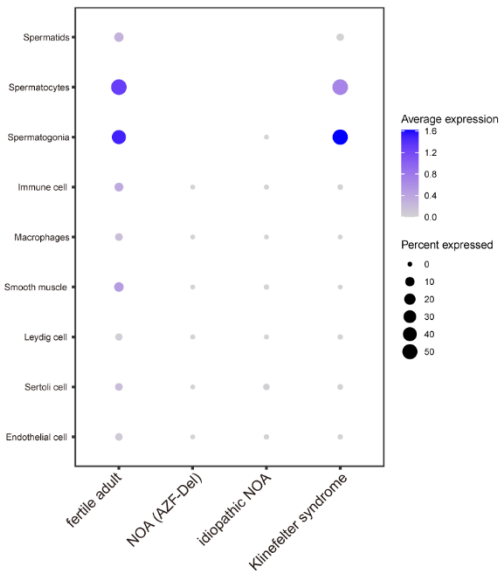

Fig. S8. Comprehensive analysis of RBM46 eCLIP targets with YTHDC2 binding sites. (A) Venn diagram depicting the overlap between RBM46 eCLIP targets and YTHDC2-bound mRNA targets identified by RIP-seq (*28*). A total of 4413 genes with RBM46 eCLIP peaks shared in two RBM46 eCLIP-seq replicates were identified ($P \leq 0.001$, fold change ≥ 8). (B) The overlap between RBM46 eCLIP targets and MEIOC RIP-seq targets. (C) Pie chart depicting the overlap between RBM46 binding sites by eCLIP and adult YTHDC2 CLIP targets within a 100-nt and 70-nt window, respectively. (D) Gene ontology analysis of common mRNAs co-targeted by both RBM46 and YTHDC2. (E) YTHDC2-binding motifs predicted by HOMER analysis from FLAG CLIP-seq in P14 FLAG-tagged *Ythdc2* mice. (F) U-rich motifs were present within a 100-nt window flanking the RBM46 motif. The top three motifs with the most significant *P*-value were shown. (G) RIP-qPCR analysis of YTHDC2 recruitment at the previously-determined sites in wild type and *Neurog*-cre *Rbm46* KO mice at P10-P12. n=6-8 for each genotype. *** $P < 0.001$, Student's t test. (H) Single-cell expression profiling of human *Rbm46* transcripts using a published single-cell datasets. Human cells were derived from fertile adults with normal spermatogenesis (fertile adults), NOA patients with Y chromosome AZF deletion (AZF-Del), idiopathic NOA patients, and NOA patients with Klinefelter syndrome.